

SMD3.pdf

Three-dimensional surface recovery with a regularized multi-frame phase shift algorithm

Fuqin Deng^{1,2} and Edmund Y. Lam¹

¹Imaging Systems Laboratory, Department of Electrical and Electronic Engineering, University of Hong Kong, Pokfulam Road, Hong Kong

²ASM Assembly Automation Ltd., Kwai Chung, Hong Kong
{fqdeng, elam}@eee.hku.hk

Abstract: We develop a modified four-frame phase shift algorithm that incorporates a smoothness constraint. This is applied to a high-precision full-profile reconstruction and measurement for integrated circuit packages.

© 2011 Optical Society of America

OCIS codes: 110.6880, 150.3040, 120.6660.

1. Introduction

In many industrial inspection systems, it is desirable to have a high-precision surface profile of the three-dimensional object without any mechanical contact. Several imaging architectures and algorithms have been developed in this regard, including shape from shading [1] and confocal imaging [2]. Here we describe our technique that falls into the realm of phase measuring profilometry (PMP) [3, 4]. It is a structure light based 3D surface signal reconstruction algorithm, and we have applied it for integrated circuit package inspections.

2. Four-frame phase shift algorithm

Consider the setup given in Figure 1. Illumination goes through the sinusoidal grating and arrives at point D on the object surface to be inspected, which is then reflected to the camera. From the camera's perspective, this ray of light would have originated from point C if the object were absent. Overall, the phase of the sinusoidal pattern reaching the camera varies according to the height of the object. When the projecting and imaging systems are both telecentric, the relationship between the surface height $h(x, y)$ and the corresponding phase offset, denoted by $\phi_h(x, y)$, is given by

$$\phi_h(x, y) = \frac{2\pi(\tan \alpha + \tan \beta)}{P} h(x, y), \quad (1)$$

where α and β are the incident angles of the projector and the camera respectively, and P is the pitch of the grating on the reference surface [3].

This phase offset, when added to a reference surface phase $\phi_r(x, y)$, becomes the total phase of the sinusoidal signal at (x, y) , denoted $\phi(x, y)$. In short, $\phi(x, y) = \phi_r(x, y) + \phi_h(x, y)$. Now if we assume $B(x, y)$ is the background intensity and $F(x, y)$ is the fringe contrast, the captured image $I_1(x, y)$ is given by

$$I_1(x, y) = B(x, y) + F(x, y) \cos \phi(x, y) + N_1(x, y), \quad (2)$$

where $N_1(x, y)$ is additive noise. The subscript "1" is there because this is the first image we would obtain. In this equation, we have three variables, namely $B(x, y)$, $F(x, y)$, and $\phi(x, y)$. Thus, we need at least three images to solve for them. In practice, it is common to use four, with phase shifts at $\pi/2$ apart. We therefore have the following three additional acquired images, i.e.

$$\begin{aligned} I_2(x, y) &= B(x, y) + F(x, y) \cos[\phi(x, y) + \pi/2] + N_2(x, y), \\ I_3(x, y) &= B(x, y) + F(x, y) \cos[\phi(x, y) + \pi] + N_3(x, y), \\ I_4(x, y) &= B(x, y) + F(x, y) \cos[\phi(x, y) + 3\pi/2] + N_4(x, y). \end{aligned} \quad (3)$$

SMD3.pdf

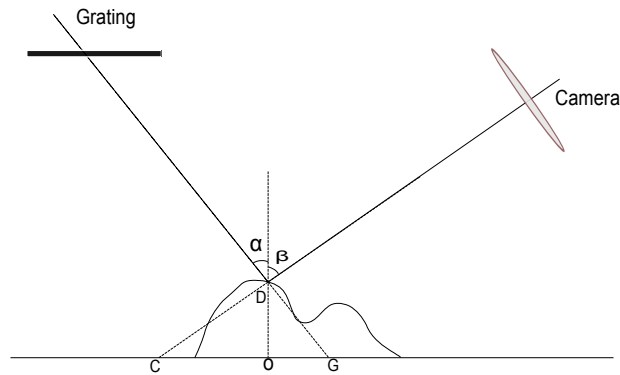


Fig. 1. The setup for the 3D phase reconstruction system.

In the absence of noise, the above equations imply that

$$\tan \phi(x, y) = \frac{I_4(x, y) - I_2(x, y)}{I_1(x, y) - I_3(x, y)}, \quad (4)$$

and therefore we have

$$\phi_h(x, y) = \arctan \left\{ \frac{I_4(x, y) - I_2(x, y)}{I_1(x, y) - I_3(x, y)} \right\} - \phi_r(x, y). \quad (5)$$

The surface height is then recovered with Equation 1.

3. Regularized four-frame phase shift algorithm

The above analytical solution is insufficient in the presence of noise. Let

$$\hat{I}_1(x, y) = B(x, y) + F(x, y) \cos \phi(x, y). \quad (6)$$

Compared with Equation 2, essentially we attempt to find $B(x, y)$, $F(x, y)$, and $\phi(x, y)$, on a pixel-by-pixel basis, such that $\hat{I}_1(x, y)$ is as close to $I_1(x, y)$ as possible. Let the difference be

$$E_1 = \|I_1(x, y) - \hat{I}_1(x, y)\|_2^2 = \sum_x \sum_y (I_1(x, y) - \hat{I}_1(x, y))^2. \quad (7)$$

The four-frame phase-shift algorithm is then to minimize $E_1 + E_2 + E_3 + E_4$, where the other terms are computed in an analogous manner.

Putting this in an optimization framework rather than the analytical form given in the last section has several advantages. First is that we can now incorporate additional constraints. We observe that the fringe contrast $F(x, y)$ is nearly constant on a homogeneous surface. As such, it is desirable to regularize this variable. Let $R(x, y)$ be the “edge image” of $F(x, y)$, which can be obtained by passing it through a high pass filter. We then seek to minimize

$$E_1 + E_2 + E_3 + E_4 + \lambda \|R(x, y)\|_2^2. \quad (8)$$

Second, as an intermediate step, we often do not treat $\phi(x, y)$ as the unknown variable, but separate it into two unknowns, namely, $\cos \phi(x, y)$ and $\sin \phi(x, y)$. This helps to take care of the nonlinearity due to the cosine function when we try to recover $\phi(x, y)$ during the optimization steps. In fact, in the noise-free case, they are given by, respectively,

$$\cos \phi(x, y) = \frac{I_1(x, y) - I_3(x, y)}{2F(x, y)} \quad \text{and} \quad \sin \phi(x, y) = \frac{I_4(x, y) - I_2(x, y)}{2F(x, y)}, \quad (9)$$

and Equation 4 follows naturally. Unfortunately, when we derive the sine and cosine as two variables, there is no guarantee that the sum of their squares equals to unity. Thus, in an optimization setting, we can add the constraint

$$[\cos \phi(x, y)]^2 + [\sin \phi(x, y)]^2 = 1 \quad (10)$$

SMD3.pdf

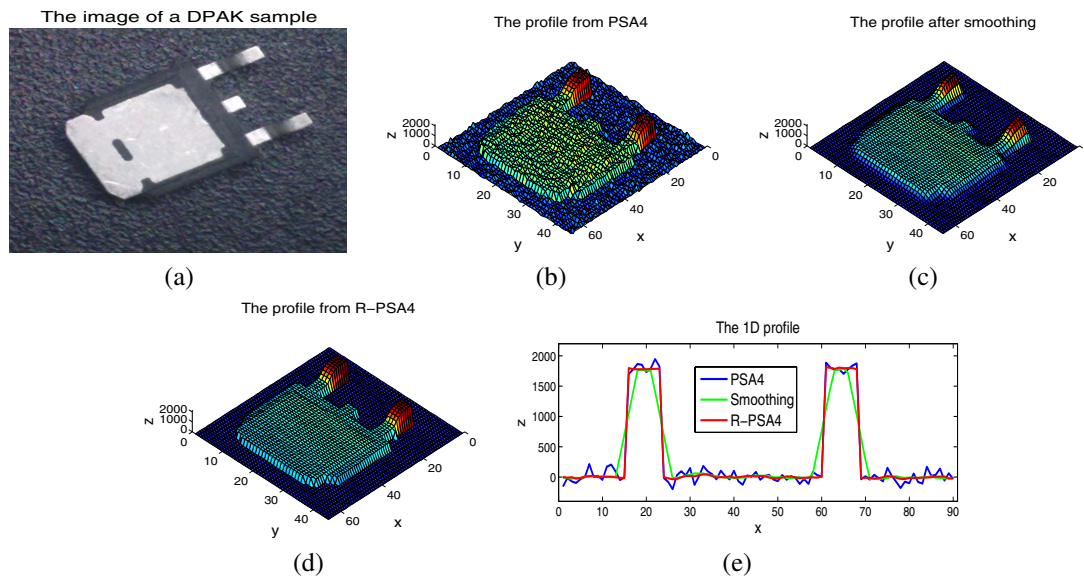


Fig. 2. (a) The image of a typical DPAK sample from the semiconductor assembly line; (b) The reconstructed profile based on PSA4; (c) The reconstructed profile by smoothing directly the profile based on PSA4; (d) The reconstructed profile based on R-PSA4; (e) The comparison of the cross-section profile reconstruction on the column with $x = 13$.

for any pair of $\{\cos \phi(x, y), \sin \phi(x, y)\}$ found in the optimization process.

Third, depending on the noise type, it is also possible to use different norm measures in both the data fidelity term (Equation 7) and the regularization term (Equation 8). A common alternative choice is the ℓ_1 norm, which is chosen for robustness to guard against outliers from intensity fluctuations and spurious reflections.

4. Experimental Results

We test the minimization with the constraints mentioned above in several integrated circuit package inspections. Figure 2 shows one such result with a discrete package (DPAK) sample, a photograph of which is given in (a). The reconstruction with the traditional four-frame reconstruction, labeled PSA4, is given in (b). As can be expected, the pixel-by-pixel reconstruction gives an image that appears quite rough; passing it through a smoothing filter gives the image shown in (c). In comparison, the reconstruction with the algorithm presented here (labeled R-PSA4) is given in (d). A cross-sectional comparison of these three images are given in (e). It can be seen that the result from our reconstruction scheme is closest to the true surface profile.

5. Conclusions

In this paper we provide a regularized scheme for the phase shift algorithm that can be used in non-contact profilometry. We incorporate a smoothness constraint and achieve reconstructed results that are closer to the true surface.

References

1. G. Zeng, Y. Matsushita, L. Quan, and H.-Y. Shum, "Interactive shape from shading," in "Computer Vision and Pattern Recognition," (2005), pp. 343–350.
2. M. Ishihara and H. Sasaki, "High-speed 3D shape measurement using a non-scanning multiple-beam confocal imaging system," in "Laser Interferometry IX: Techniques and Analysis," , vol. 3478 of *Proceedings of the SPIE* (1998), pp. 68–75.
3. V. Srinivasan, H. Liu, and M. Halioua, "Automated phase-measuring profilometry of 3-D diffuse objects," *Applied Optics* **23**, 3105–3108 (1984).
4. X. Su and W. Chen, "Fourier transform profilometry: A review," *Optics and Lasers in Engineering* **35**, 263–284 (2001).